INTERNATIONAL JOURNAL FOR NUMERICAL METHODS IN FLUIDS
Int. J. Numer. Meth. Fluids 2002; **38**:1027–1044 (DOI: 10.1002/fld.252)

A simplified quasi-two-dimensional model for gain optimization in carbon dioxide gasdynamic lasers (GDL)

A. R. Bahrampour[1,2,*], R.-M. Farrahi[1,2] and M. Radjabalipour[1]

[1] *Kerman University, Kerman, Iran*
[2] *University of Rafsandjan, Kerman, Iran*

SUMMARY

In this paper a simplified quasi-two-dimensional model for small signal gain optimization in gasdynamic laser is introduced. In order to obtain a homogeneous medium with maximum optical gain in the active medium, by nozzle shape formation, the shock occurrence position is controlled and is postponed to some point behind the laser active medium. Then the method of calculus of variation is used to find the supersonic part of the nozzle of a gasdynamic laser with maximum gain in the active medium. The interesting result is that the supersonic part of such a nozzle consists of a wedge as the accelerating part of the nozzle, a smooth surface for the uniformization, and finally a channel for the relaxation of the medium. (The middle section is characterized as the geometrical locus of points whose characteristic curves are concurrent at a certain point.) It is also shown that, overlooking a minor difference in the gain, the nozzle can be chosen to be a shock free one with the ultimate optical uniformity. Copyright © 2002 John Wiley & Sons, Ltd.

KEY WORDS: lasers (CO_2); gasdynamic lasers; gain optimization

1. INTRODUCTION

Carbon dioxide gasdynamic lasers (GDLs) as sources of high-power infrared coherent radiation are interesting both from theoretical and experimental point of view. In these lasers the population inversion is achieved via rapid cooling of heated laser gases such as (CO_2–N_2–H_2O) or quick heating of cooled laser gases. Our interest is in the former type in which either the hot laser gas is produced from a combustion process, or laser gas mixture has been heated directly by an electrical arc heater [1]. For the sake of simplicity, suppose that the molecules of the active medium act as two-level quantum systems and the propagating light in the medium is tuned to atomic line centre, i.e. the difference in the energies of the atomic levels is equal to the energy of each photon of the light beam. The lower and the upper energy levels of the molecules are called, respectively, the lower and the upper

*Correspondence to: A. R. Bahrampour, Physics Department, Vali-Asr University, Ghaffari Square, P.O. Box 77139-518, Rafsandjan, Iran.

Contract/grant sponsor: ICST, Kerman, Iran
Contract/grant sponsor: ICTP, Triest, Italy

Received 14 July 1999
Revised 22 January 2001

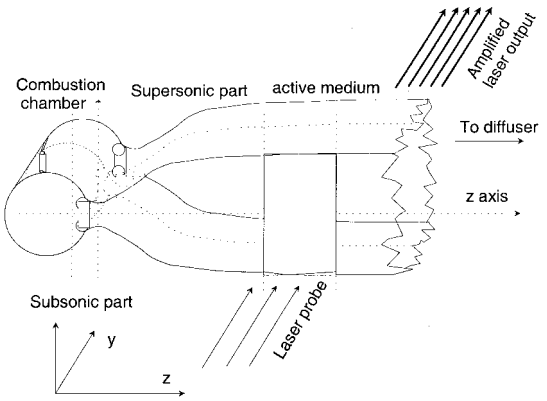

Figure 1. The schematic of a gas-dynamic laser. These lasers generally consist of four distinct parts, which are, combustion chamber, supersonic nozzle, active medium, and diffuser.

laser levels. The number of photon absorption is proportional to the number of atoms in the lower energy level, and the number of stimulated emissions is proportional to the number of atoms in the upper laser level. Assuming Boltzmann distribution for equilibrium, it follows that when a collection of atoms is in thermal equilibrium, upper-level population is always less than lower-level population. Total stimulated-transition rate on such systems is thus absorptive or attenuating rather amplifying. To create laser amplification, we must find some pumping process which results more atoms in upper laser level than lower level. Such pumping process causes a non-equilibrium state for the system which is called population inversion state.

In the heated laser gas mixture the population of both the upper and lower laser levels are considerable but yet the population of the lower laser level is greater than that of the upper laser level. The heated gas mixture then flows through a supersonic nozzle (Figure 1) which forces the translational temperature and the pressure to drop to a low value.

Suppose that, as it is true for some vibrational states of the CO_2 molecule, the lifetime of the upper laser level is large compared with that of the lower laser level and the gas expansion time. This implies that the lower laser level population relaxes faster than that of the upper laser level. In other words, vibrational temperature of the lower level is close to the translational temperature while the vibrational temperature of the upper level is nearly equal to the reservoir temperature. In this way, the population inversion would be achieved. Since the rate of cooling and relaxation of the laser levels depends on the nozzle shape, in such lasers the population inversion, and hence the gain in the active medium, depends not only on the gas parameters in the reservoir but also on the supersonic nozzle shape as well. It is common to characterize a nozzle by the ratio of the area $A(z)$ of each cross-section to that of the nozzle at the critical section ($A^* = A(0)$) as a function of the distance z of the section from the throat. The function is called the nozzle shape or area ratio and is denoted by $a(z) = A(z)/A^*$ (Figure 2).

Theoretical gain optimization versus the nozzle shape has been carried out by several investigators [1–11]. Losev and Makarov [2] have considered a planar wedge nozzle shape of

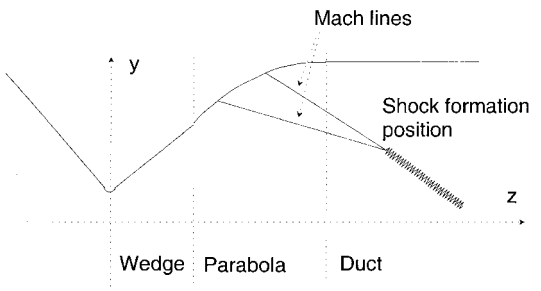

Figure 2. The nozzle shape which is the upper part of the intersection of a planar supersonic nozzle with the y–z plane and is normalized to the throat height. The x–z plane is the symmetric plane of the planar nozzle.

the form

$$a(z)=\begin{cases}1+az & \text{for } 0\leqslant z\leqslant l\\ 1+al & \text{for } l\leqslant z\leqslant L\end{cases} \tag{1}$$

which has three parameters a, l, and L. Here $a=2\tan\theta/h^*$ is the slope of the wedge, θ is the inclination angle, l is the length of the wedge part of the nozzle, and L is the total length of the nozzle (the distance from the nozzle throat to the point at which the maximum gain is obtained). Optimization is carried out versus these parameters. Reddy and Shanmugasundaram [5–7] used nozzles defined by $a(z)=(1+z^j)^i$ where i and j are positive integer numbers. Biryukov *et al.* [8] carried their optimization for the nozzle profile

$$a(z)=\begin{cases}1+a\log(bz+1) & \text{for } 0\leqslant z\leqslant l\\ 1+a\log(bl+1) & \text{for } l\leqslant z\leqslant L\end{cases} \tag{2}$$

versus a, b, l, and L. Here $ab=2\tan\theta/h^*$, $H=(1+a\log(bl+1))$ is the expansion ratio, h^* is the height of the throat cross-section, θ is the maximum expansion angle, l is the length of the curved part of the nozzle, and L is the total length of the nozzle. A more general numerical parametric family of nozzles has been used by Losev and Makarov [3]. They divided the nozzle into n sections and each section was approximated by a parabola of the form $a(z)=a_iz^2+b_iz+c_i$, $z_i\leqslant z\leqslant z_{i+1}$. Then by applying the continuity of nozzle shape and its first derivative, the optimal nozzle's parameters (a_i,b_i,c_i) were calculated. In each of the works mentioned above, the gain optimization problem was reduced to a multi-parametric optimization problem and the optimal nozzle was the best among the selected family. The authors of Reference [9] chose a non-parametric approach; they used the Pontryagin's maximum principle to find an optimal shape among all smooth monotone functions $a(z)$. In Reference [9], the oblique shocks were avoided by assuming the shape of the nozzle is smooth. Also, the curved shocks were hoped to be postponed to a point outside the active media by imposing a lower bound on the curvature of the nozzle shape. In this way the model was reduced to a quasi-one-dimensional model. The shape of the nozzle is thus obtained as a combination of three surfaces: the acceleration part is a wedge; the uniformization part is a parabolic surface; the relaxation part is a duct.

Practically, the oblique and curved shocks cause losses in the maximum gain and the optical uniformity of the active medium. Thus, it is interesting to study the full behaviour of the shocks. In the present paper we try to expel the shocks from the active medium by determining the point outside the nozzle at which the shocks occur for the first time. For this, we can no longer assume a quasi-one-dimensional model and, in fact, a quasi-two-dimensional model is employed. If L is the length of the nozzle and z_1 is the first point at which the shocks occur, we set $\alpha = L/z_1$. The parameter α with constraints $0 \leqslant \alpha \leqslant 1$ plays an important role in the optimization process. It is shown that α must be 1 to obtain the highest gain. But in this case the optical uniformity is disturbed. On the other extreme, for the perfect optical uniformity, α must be 0. In this case, not only the loss in gain is insignificant, but also the nozzle shape is the well-known shock-free nozzle ($z_1 = \infty$). In general, optimal shape of the supersonic part consists of a wedge, and a channel joined by a smooth surface, along which the Mach lines are concurrent at z_1.

2. FORMULATION OF THE STATE VARIABLE EQUATIONS AND CONSTRAINTS

Throughout the paper, the gas mixture will consist of CO_2, N_2, and H_2O. It is assumed the nozzle has a non-equilibrium one-dimensional steady-state inviscid ideal gas flow with no changes in its chemical composition. The governing equations of the flow are

$$\rho v A = q \tag{3}$$

$$\mathrm{d}P/\rho + \mathrm{d}v = 0 \tag{4}$$

$$v^2/2 + R\gamma(\gamma - 1)^{-1}T + e_1(T_1) + e_2(T_2) = H_0 \tag{5}$$

$$P = \rho R T \tag{6}$$

where q is the mass flux of gases.

The first three equations are continuity relations for mass, momentum and energy, respectively; the last equation is the state equation for an ideal gas.

In quasi-one-dimensional models, it is assumed that the physical quantities remain constant throughout each section of the active medium perpendicular to the flow axis; this is why the boundary layers, wake, and the shock wave effects were ignored [12]. In our model, which is quasi-two-dimensional, although the shock waves are present, but we expel them from the active medium.

A second set of equations must be considered, that represents the translational–vibrational ($T - V$) and vibrational–vibrational ($V - V$) energy transfers between the vibrational modes of N_2 and the symmetric bending and anti-symmetric vibrational modes of CO_2. To simplify the analysis we will use the Anderson's bimodal vibrational model [1]. In this model the upper laser level ((001) of CO_2) is in thermal equilibrium with $v = 1$ level of N_2. In each vibrational model, levels of a mode are in thermal equilibrium and also obey the Boltzmann distribution with the corresponding vibrational temperature of the mode. A schematic of the vibrational model is shown in Figure 3. In this figure, mode I (of vibrational temperature T_1) and mode II (of vibrational temperature T_2) include, respectively, the lower and the upper

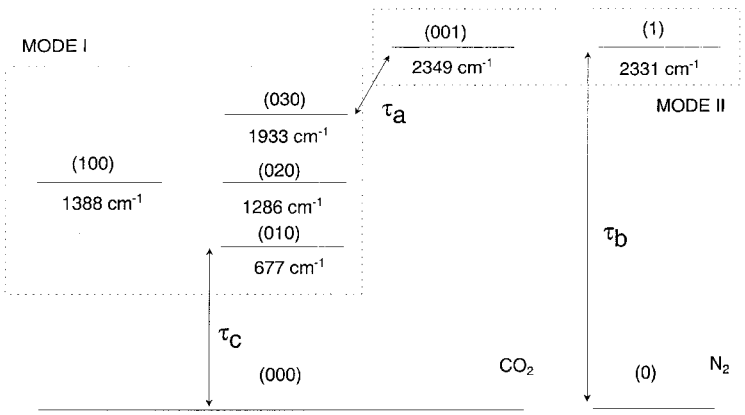

Figure 3. The Anderson's bimodal vibrational model used in the calculations of this paper. The lower and upper laser levels belong to the modes I and II, respectively.

level of the laser system and also some other dominant levels. τ_a, τ_b, and τ_c are the time constants of the relaxation processes of these modes.

Each mode can be considered as a simple harmonic oscillator, and the relaxation equations of two vibrational modes can be written as follows [13]:

$$\frac{\mathrm{d}e_i}{\mathrm{d}z} = \frac{e_i(T) - e_i(T_i)}{\tau_i v} \quad (i = 1, 2) \tag{7}$$

Since the sharp corners in the nozzle shape cause the oblique shock formation, in this investigation the continuity of the nozzle shape and its first derivative are assumed.

For very large divergence angles, not only the one-dimensional nature of the flow is violated, but also the possibility of shock wave formation and separation of the flow from the walls arises. Throat height h^* is restricted from below by the boundary layer effects [12]. Hence in our calculation an upper bound for the slope of the nozzle shape is assumed. Also, to terminate into a channel with a quasi uniform flow, we further assume that the slope is non-negative and its first derivative is non-positive everywhere.

In particular, we have

$$0 \leqslant x_5 \leqslant \beta \tag{8}$$

$$u \leqslant 0 \tag{9}$$

where $x_5(z)$ is the slope of the nozzle shape at point z and β is its upper bound. For a concave downward nozzle shape, the second derivative $u(z) = \mathrm{d}x_5/\mathrm{d}z$ is negative.

Shock waves introduce not only discontinuities or rapid changes in the thermodynamical variables such as density of the gas mixture and pressure, but also influence the optical refraction coefficient of the gas mixture in the active medium. Therefore, the occurrence of the shock waves, in the active media and in the immediate area, destroys the optical uniformity and the gain coefficient. So to develop a more uniform active media it is necessary to postpone the shock wave formation to a region far enough from the end of the nozzle. But since the oblique and curved shocks formation are two-dimensional phenomena, a two-dimensional

non-equilibrium model for their analysis is necessary. Losev and Makarov have used such a model for numerical study of two-dimensional behaviour of a supersonic wedge nozzle [4]. Anderson's time dependent method as well as the characteristic method are commonly used in the analysis of the gas flow in a two-dimensional supersonic nozzle.

Analysis of a nozzle flow can be carried out by either direct or reverse approach. In the direct approach, the nozzle contour is given, and we must determine the distribution of all gasdynamic and optical parameters in the medium. On the contrary, in the reverse approach, it is required to find a contour for the nozzle such that one of gain, output power, etc., is maximized at the exit, or the distribution of a certain parameter like temperature, pressure, etc. follows a given formula. Hence our task in this paper, to optimize the gain via the nozzle shape in shock free active medium situation, is a reverse problem.

The oblique and curved shocks usually start from the intersection point of two nearest characteristic curves of the same family. To reduce the CPU time and to simplify the physical model, we approximate the non-equilibrium characteristic curves by the Mach lines of the equilibrium flow. Due to this approximation, the method is called a quasi-two-dimensional one. It follows from this approximation that the curved shock waves occur at the position z_s of the intersection point of two close Mach lines starting from the points z and $z+\mathrm{d}z$. There is a position z_s corresponding to each point z along the supersonic part of the nozzle which is determined via $z_s = z_s(z, x(z), u(z)) = z + 1/[h_1(z,x)u + h_2(z,x)]$, where x stands for certain independent variables to be introduced later (see Appendix B). For the expansion wave, the intersection of Mach lines is at some point preceding to the position z, and hence $z_s \leqslant z$ which causes no shock wave. For the compression wave, to avoid the curved shock waves in the active media, z_s must be well out of the active media and this can be achieved by setting some restrictions such as $z_s \geqslant (1/\alpha)L$ for all z in the compression zone and for a certain constant $\alpha (0 \leqslant \alpha \leqslant 1)$ independent of z. The situation in the expansion zone as well as the requirement in the compression zone can be formulated in a single formula as follows:

$$h(z,x,u,L) = (z_s - z)(\alpha^{-1} z_s - L) \leqslant 0 \tag{10}$$

Let us now introduce the vector x called the state vector. For each z, define $x \in \mathbb{R}^5$ by

$$\begin{aligned} x^{\mathrm{T}}(z) &= (x_1(z), x_2(z), x_3(z), x_4(z), x_5(z)) \\ &= (T_1(z), T_2(z), T(z), a(z), \mathrm{d}a/\mathrm{d}z) \end{aligned}$$

where the superscript T stands for the transpose of a vector. Then, one can write the governing equations (3)–(7) in a standard form, called the state equation, which is suitable for calculus of variation or optimal control theory:

$$\dot{x}^{\mathrm{T}} = (\dot{x}_1, \dot{x}_2, \dot{x}_3, \dot{x}_4, \dot{x}_5) = (x_4^{-1} f_1, x_4^{-1} f_2, x_4^{-1}(f_4 x_5 + f_3), x_5, 0) \tag{11}$$

$$+ (0,0,0,0,1)u = F(x) + bu \tag{12}$$

where $F(x) = (x_4^{-1} f_1, x_4^{-1} f_2, x_4^{-1}(f_4 x_5 + f_3), x_5, 0)$ and $b = (0,0,0,0,1)$.

Hence, the optimization problem reduces to an open-loop optimal control problem where the small signal gain of the active medium is the cost function and the second derivative of the nozzle shape ($u = \mathrm{d}^2 a/\mathrm{d}z^2$) is the open-loop control variable. The functions f_i ($i = 1,2,3,4$)

are differentiable and their exact forms are given in Appendix A. The initial values of the state variables x_1, x_2, and x_3 at $z = 0$ are determined by the reservoir conditions and the subsonic structure of the nozzle, and that of x_4 is equal to 1. The initial value of x_5 is $x_5(0) = (2/h^*)\tan(\theta/2)$ where h^* is the throat height and θ is the opening angle. The value of $x_5(0)$ will be determined in the optimization process. The problem is now to optimize the small signal gain $g_0 = g_0(x_1, x_2, x_3)$ (see Appendix A for detail), where x_1, x_2, x_3 satisfy the state equations (12) with constraints (8)–(10) and certain particular initial conditions.

3. GAIN OPTIMIZATION WITH RESPECT TO THE NOZZLE SHAPE

Now, the gain optimization problem is the optimization of the small signal gain with respect to the second derivative of the nozzle shape, which is called control and is denoted by u, with two set of equality and inequality constraints. The set of equality constraints is set (12) of certain first-order ordinary differential equations. By introducing new variables q_1, q_2, and q_3 which are some unknown functions of z, the set of inequality constraints (8)–(10) can also be written as the following equality constraints:

$$x_5(x_5 - \beta) + q_1^2 = 0 \tag{13}$$

$$h(z, x, u, L) + q_2^2 = 0 \tag{14}$$

$$u + q_3^2 = 0 \tag{15}$$

In vector notation the above equations can be rewritten as follows:

$$y^{\mathrm{T}} = (x_5(x_5 - \beta) + q_1^2, h(z, x, u, L) + q_2^2, u + q_3^2) = 0 \tag{16}$$

Now we can combine all these equations by means of Lagrange multipliers. Since Equations (12) and (16) must be satisfied for all position z from 0 to L, a Lagrange multiplier for each value of z must be used and hence Lagrange multipliers are also functions of z.

Let the vector functions $\mathbf{p} = (p_1, p_2, p_3, p_4, p_5) \in \mathbb{R}^5$ and $\lambda = (\lambda_1, \lambda_2, \lambda_3) \in \mathbb{R}^3$ be the Lagrange multipliers corresponding to the state equations (12) and constraints (16), respectively. Now, the optimization problem reduces to optimize the following generalized cost function without any constraints:

$$g_a = g_0(x(L)) + \int_0^L [p^{\mathrm{T}}(F(x) + bu - \dot{x}) + \lambda^{\mathrm{T}} y]\, \mathrm{d}z \tag{17}$$

Applying the variational method [16], the equation $\delta g_a = 0$ for the optimal case yields

$$\lambda_i q_i = 0 \quad (i = 1, 2, 3) \tag{18}$$

$$y = 0 \tag{19}$$

$$p^{\mathrm{T}} b + \lambda_2 \frac{\partial h}{\partial u} + \lambda_3 = 0 \tag{20}$$

$$\dot{x} = F(x) + bu \tag{21}$$

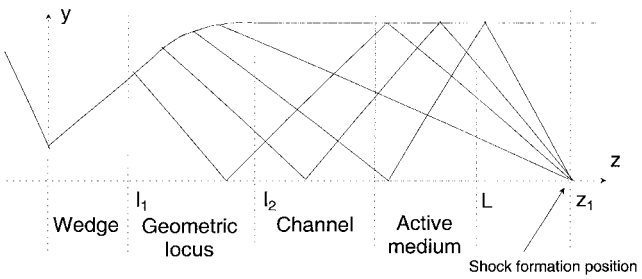

Figure 4. Schematic of the characteristic curves in a maximum gain nozzle shape for a gasdynamic laser. l_1, l_2, and L are, respectively, the end position of the accelerating part, the uniformization part, and the nozzle. z_1 is the shock formation position.

$$\dot{p}^{\mathrm{T}} = -\left(p^{\mathrm{T}} \frac{\partial F}{\partial x} + \lambda_2 \frac{\partial h}{\partial x} + \lambda_1 b^{\mathrm{T}} (2x_5 - \beta) \right) \tag{22}$$

$$(p^{\mathrm{T}}(F(x) + bu) + \lambda^{\mathrm{T}} y)|_{z=L} + \int_0^L \frac{\alpha^{-1}\lambda_2}{(h_1 u + h_2)} \, \mathrm{d}z = 0 \tag{23}$$

$$p(L) = \left. \frac{\partial g_0}{\partial x} \right|_{z=L} \tag{24}$$

The optimal solution is now obtained by solving (18)–(24) for x, p, λ, q, and u. If $q_1 = 0$ for all z in some interval, then it follows from (16) that either $x_5 = \beta$ or 0 which yields a wedge or a channel, accordingly. In both cases $u = 0$. For the remainder of the nozzle, we proceed as follows. If λ_2 or λ_3 is non-zero on some interval, then u is determined by either $u = 0$ or $h(z, x, u, L) = 0$. If $u = 0$, the concerned part of the nozzle is again either a wedge or a channel. If $h = 0$, then $z_s = \alpha^{-1} L$ and hence z_s is constant on that interval, i.e. all Mach lines pass through the same point which is denoted by z_1. Finally, if λ_2 and λ_3 vanish simultaneously on an interval, then we face singularity and hence u cannot be determined directly. In this case, using Equation (20) and its first and second derivatives with respect to z, the optimal control u can be determined at each point of singularity as a function of the state variable x, i.e. $u = u_s(x)$ with $u \leqslant 0$ and $h(z, x, u, L) \leqslant 0$ (see Appendix C for detail).

Summing up, in the absence of singularity, and in view of the fact $u \leqslant 0$, the following assertions are true in the optimal case:

- The Channel part will occur only at the end part of the nozzle.
- Due to the smoothness of the shape function the wedge and the channel cannot be adjacent.
- Since $\mu = \sin^{-1}(1/M)$ is decreasing and since the Mach lines initiating from the curved parts all pass through the same point $z_1 = \alpha^{-1} L$, it follows that disjoint wedge parts do not occur.
  (Here $M = v/\sqrt{\gamma RT}$ is the freezing Mach number and μ is the angle between the stream line and the Mach line.)

Thus, the nozzle is divided into three distinct parts (as shown in Figure 4). The first part is a wedge, the second part is a curved surface with the property that all Mach lines concurred

at the point $\alpha^{-1}L$, and the third part is a channel. As is the case in a general gasdynamic laser, the supersonic part of the nozzle is composed of three parts: the first part is the acceleration region for rapid cooling of the laser gases, the second part is the uniformization zone, and finally the third part is the relaxation region for the lower level of laser. Theoretically, one may argue that the wedge part or the channel part may vanish, and the rapid cooling or relaxation occur in the middle part.

However, the optimal nozzle shape depends on a set of numerical parameters $l_1, L, x_5(0)$, in which l_1 is the end of the wedge part. Note that the end of the curved part l_2 is not an independent parameter and is determined by the equation $x_5(l_2) = 0$. To find the exact shape of the optimal nozzle, we must now solve a multi-factor optimization problem by the numerical methods [2].

4. GENERAL RESULTS

In the previous section by specifying the second derivative of the optimal nozzle shape, the family of maximum gain nozzles is specified and it is shown that it belongs to the following class of functions:

$$u = \begin{cases} 0 & 0 \leqslant z \leqslant l_1 \\ h_3(z) = \dfrac{1 - (\alpha^{-1}L - z)h_2(z,\ x(z))}{(\alpha^{-1}L - z)h_1(z,\ x(z))} & l_1 \leqslant z \leqslant l_2 \\ 0 & l_2 \leqslant z \leqslant L \end{cases} \tag{25}$$

This family of nozzles is characterized by the parameters L, l_1, l_2, α where l_1 is the length of the accelerating part. $l_2 - l_1$ is the length of the uniformization region, L is the total length of the supersonic nozzle, and α is a characteristic parameter for the optical uniformity of the active medium and is chosen in laser design procedure. Upon the continuity requirement of the nozzle shape and its first derivative, l_2 can be determined with respect to other parameters and is not an independent variable. Hence the nozzle can be specified by only three parameters.

Small signal gain depends on some other parameters such as mixture composition (X_{CO_2}, X_{N_2}, X_{H_2O}) and initial conditions (the pressure p_0 and the temperature T_0 at the nozzle entrance). In this paper, the effect of some of these parameters on the optimal gain and optimal shape parameters (l_1, $l_2 - l_1$, and L) are studied. State equations carry a singular point at sonic velocity ($M_f = 1$) in the proximity of the nozzle throat. So we seek the solution of the state equations in the region close to sonic velocity by using the transsonic approximation. Then we will determine the solutions for the adjoining upstream regions in the supersonic part from the values obtained in downstream regions [11].

We employ the Runge–Kutta method implemented in Mathematica media to compute the derivatives of the system variables x along the z-axis and then determine the state variables and the small signal gain in the active medium versus the desired parameters.

5. NUMERICAL RESULTS

Selecting the desired parameters, the solution of the state variable equations along the z-axis by means of the Runge–Kutta method is determined. Then the small signal gain optimization via

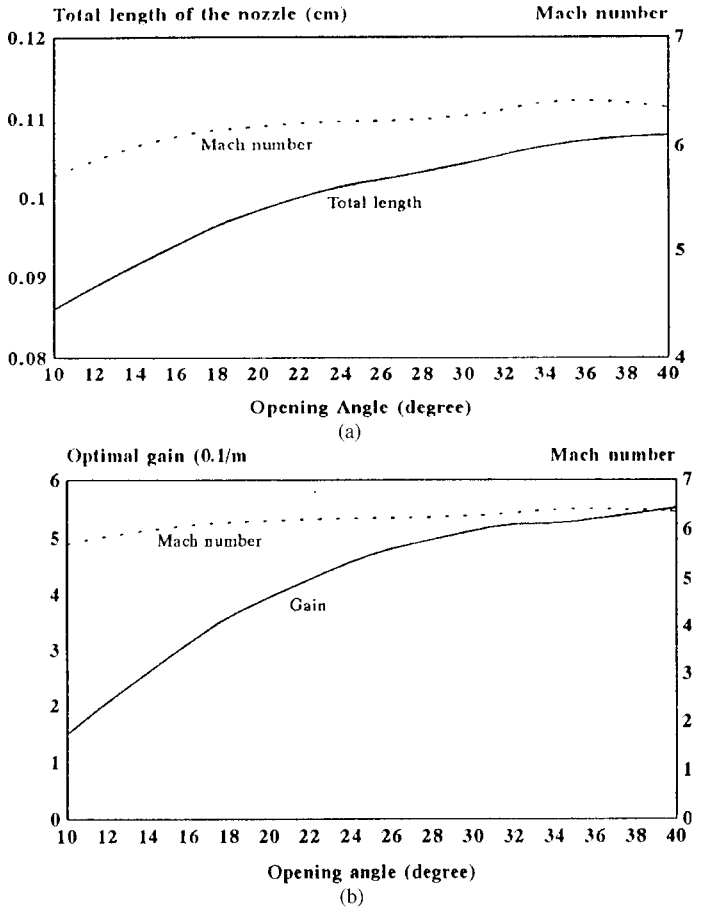

Figure 5. Optimal nozzle parameters and optimal gain versus opening angle of the supersonic part of the nozzle. (a) Total length of the optimal nozzle (in cm) and maximum Mach number in the duct. (b) Optimal gain (0.1 dB/m) versus β. ($p_0 = 20$ atm, $X_{N_2} = 0.85$, $X_{CO_2} = 0.1$, $\alpha = 0.4$.)

selected parameters is done. An upper bound is imposed on the slope of the nozzle shape to avoid the wall detachment of the gas flow, boundary layer, and wake effects. Figure 5(a) shows that the optimum gain increases as the opening angle increases. (This is a direct consequence of Pontryagin's maximum principal [9].) The figure also shows that the gain has, however, a saturation value. The saturation values are obtained when the upper and the lower laser levels freeze, respectively, to the reservoir temperature and translational temperature, i.e. in maximum non-equilibrium condition. To study the problem for the high values of the slope, two-dimensional analysis is inevitable. By two-dimensional analysis an optimal value for the slope is predicted [4]. Figure 5(b) shows that the nozzle length L increases as β increases, this is due to the increase of the maximum Mach number which causes the increase of the relaxation times of the laser levels. The difference between the vibrational temperatures at the entrance of the duct increases as β increases. For low values of β, optimum gain occurs in the

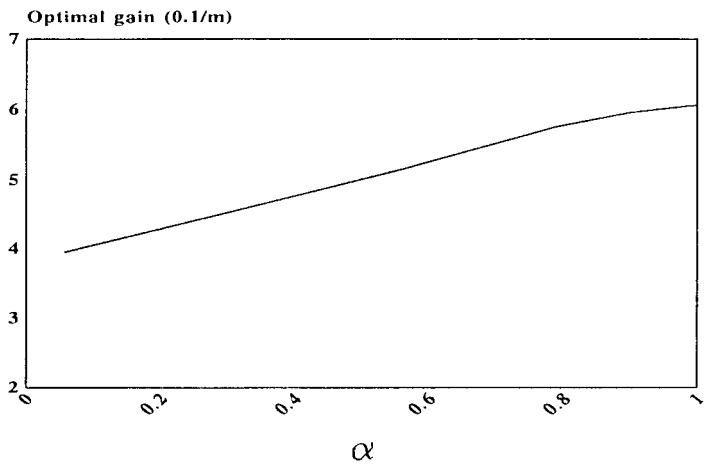

Figure 6. Optimal gain (in 0.1 dB/m) as a function of dimensionless parameter α $(=L/z_1)$. ($p_0 = 20$ atm, $X_{N_2} = 0.85$, $X_{CO_2} = 0.1$, opening angle $= 20$.)

accelerating part of the nozzle, i.e. it occurs in the wedge section of nozzle. The length of the accelerating part of the nozzle is a decreasing function of the slope of the nozzle shape while the length of the uniformization region is an increasing function of β. In all of our calculations, the non-equilibrium characteristic curves are approximated by the equilibrium Mach lines. As a result of the above approximation the total length and the length of the wedge part of the nozzle are independent of α while the length of the uniformization part decreases as α decreases. Figure 6 shows that the optimal gain decreases as the parameter α decreases. But losing a small value of gain, a great increase in uniformity of flow is achieved. Dependence of the parameters of the optimal gain nozzle on the carbon dioxide molar fraction is shown in Figure 7. For designing the supersonic part of an optimal gasdynamic laser nozzle, Figures 7(a)–(c) determine the nozzle parameters and active medium position for certain fuel types and reservoir conditions. Figure 7(d) shows the optimal gain for various values of carbon dioxide and the stagnation pressures; the behaviour is the same as in Reference [1] in which the nozzle is fixed and the gain is drawn versus the amount of carbon dioxide.

In Appendix D, we have employed a two-dimensional model for gas flow to determine the flow as well as the exact place in the nozzle at which the oblique shock wave occurs. The results are shown in Figure 8 with $p_0 = 20$ atm, $T_0 = 1220$ K, $X_{CO_2} = 0.1$, $X_{N_2} = 0.85$, $X_{H_2O} = 0.05$, $L = 0.15$ m, and $\alpha = 0.9$. The Figures 8(a)–(d), respectively, show the Mach number, the pressure, the horizontal velocity, and the vertical velocity in the nozzle. Figure 8(a) shows that the oblique shock wave is started from the point 14 cm from the throat which is almost equal to the value $z_1 = L/\alpha = 0.15/0.9 \approx 0.166$ m obtained from our quasi-two-dimensional model. Figure 8(b) shows that the pressure variations is high in the region with oblique shock waves and that the optical uniformity is low. Figure 8(c) shows the horizontal velocity from which we see that the uniformity of flow exists in the active medium. Figure 8(d) shows the variation of the vertical velocity from which we see that ignoring the vertical velocity in our quasi-two-dimensional model may cause errors in Mach number and other parameters. Finally, in Table I, the maximal gain of our optimal solution with respect to

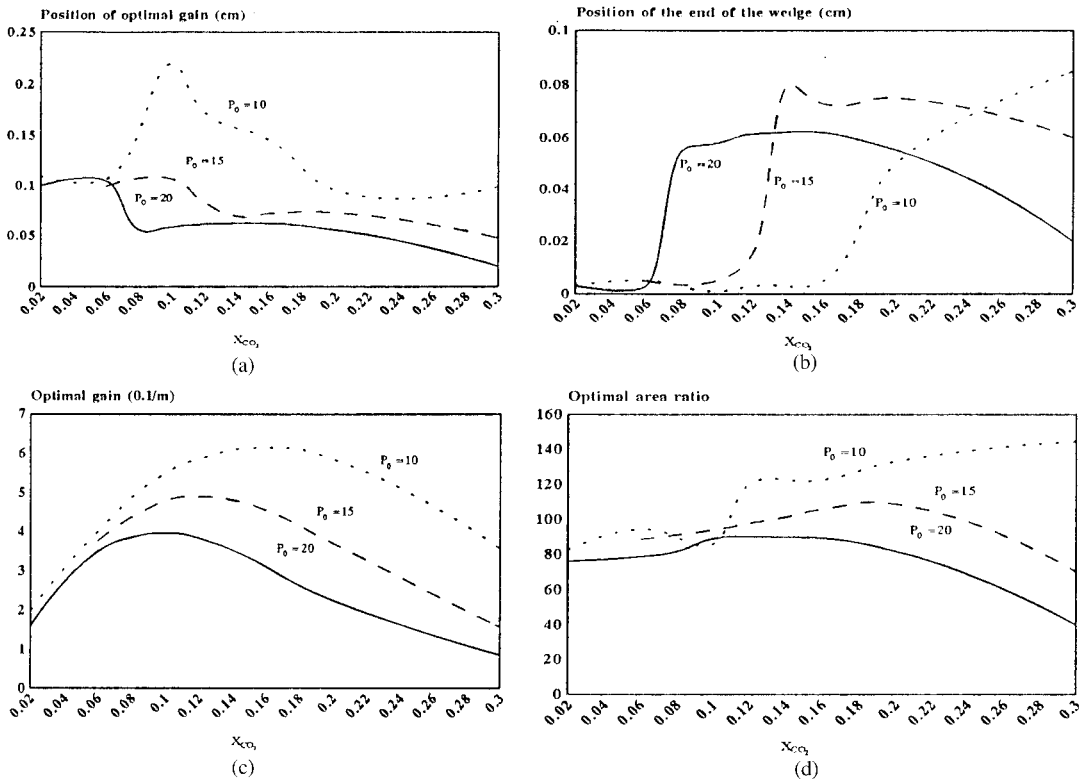

Figure 7. Optimal nozzle parameters and optimal gain versus carbon dioxide mole fraction. (a) Total length of the optimal nozzle (in cm). (b) Length of the wedge part of the optimal nozzle (in cm). (c) Maximum area ratio of the optimal nozzle. (d) Optimal gain versus X_{CO_2} (in 0.1 dB/m).

various reservoir conditions is compared with similar maximal gains of nozzles reported by others. (In all cases the CO_2–N_2–H_2O is produced through the combustion of C_6H_6–O_2–N_2 fuel.) As it is expected, the table reveals that the optimal gain of the nozzle introduced by us is the greatest. (All other nozzles are in "first generation" class of GDLs [1, p. 89]: $T_0 \simeq 1200$ K; other reservoir values, molar fractions and stagnation pressure, are determined through the optimization process.)

6. CONCLUSION

In the present work, gain optimization is done versus the supersonic nozzle shape. Our interest is in combustion driven gasdynamic lasers in which CO_2–N_2–H_2O is produced through the combustion of C_6H_6 (as fuel), O_2 (as oxidizer), and N_2. The temperature of combustion chamber is about 1200 K. Our gain as is inferred from Table I, has an increase of 18.3% over the last previous result. We have proved that supersonic part of a nozzle with maximum gain in the active medium consists of a wedge as the accelerating part of the nozzle, and

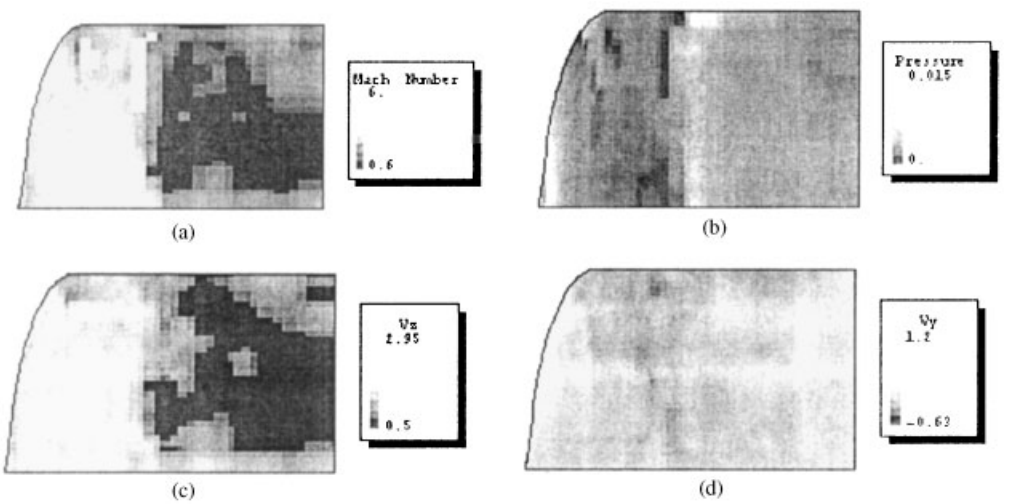

Figure 8. Two-dimensional flow fields in the nozzle. (a) Mach number, (b) pressure, (c) horizontal velocity, (d) vertical velocity. ($p_0 = 20$ atm, $T_0 = 1220$ K, $X_{CO_2} = 0.1$, $X_{N_2} = 0.85$, $X_{H_2O} = 0.05$, $L = 0.15$ m, and $\alpha = 0.9$.)

Table I.

Gain (1/m)	0.5	0.6	0.4	0.71	0.84
Nozzle shape	Planar	Circular-circle	Planar	SFML*	SFON†
Reference	[17]	[19]	[20]	[18]	Pres. Work

*SFML: Shock free minimum length nozzle.
†SFON: Shock free optimal nozzle presented in this paper.

a duct joined by a smooth surface characterized by the geometrical locus of points whose characteristic curves of the same family are concurrent at a certain point (smooth surface and duct act as uniformization and relaxation parts of the nozzle). The length of each section and the maximum area ratio of the nozzle are the nozzle parameters and strongly depend on the reservoir parameters such as stagnation pressure, stagnation temperature, and molar gas fractions.

ACKNOWLEDGEMENTS

The third author is supported by ICST (Kerman, Iran) and ICTP (Triest, Italy) as a regular associate member.

APPENDIX A

The vibrational model used in this work is the Anderson's bimodal model [1]. According to this model and the quasi-one-dimensional inviscid non-chemical reacting ideal gas flow

assumptions the functions f_i $(i=1,2,3,4)$ are as follows:

$$f_i = \frac{Q(e_i(x_i) - e_i(x_3))}{\gamma M^2 p\tau_i e_i'(x_i)} \quad (i=1,2) \tag{A1}$$

$$f_3 = \frac{Q(\gamma-1)(\gamma M^2-1)}{\gamma^2 M^2 R(M^2-1)} \sum_{i=1}^{2} \frac{e_i(x_i) - e_i(x_3)}{p\tau_i} \tag{A2}$$

$$f_4 = -\frac{(\gamma-1)M^2 x_3}{(M^2-1)} \tag{A3}$$

The gain function for non-lasing operation is given by

$$g_0 = \frac{e^{-3383/x_2} - e^{-1999/x_1}}{x_3^{3/2} e^{234/x_3}} \frac{0.0977}{Q} \frac{T_0^{3/2} X_{CO_2}}{X_{CO_2} + 0.7589 X_{N_2} + 0.3236 X_{H_2O}} \tag{A4}$$

where the energy of the ith vibrational mode and its relaxation lifetime, as a function of the state variables and gas fractions, is given in Reference [1].

APPENDIX B. CURVED SHOCK WAVES FORMATION POSITION

Oblique shock waves are two-dimensional phenomena; their formation positions are the intersection points of the characteristic curves of the governing hyperbolic partial differential equations [14, 15]. In this work we use the Mach lines as an approximation of the characteristic curves. The equations of the Mach lines which start from the points $(z, x_4(z))$ and $(z+\mathrm{d}z, x_4(z+\mathrm{d}z))$ on the boundary of the nozzle are as follows:

$$(Y - (h^*/2)x_4(z)) = (X - z)\tan(\theta - \mu) \tag{B1}$$

$$(Y - (h^*/2)x_4(z+\mathrm{d}z)) = (X - z - \mathrm{d}z)\tan(\theta - \mu + \mathrm{d}\theta - \mathrm{d}\mu) \tag{B2}$$

where $\tan\theta = A^* x_5$, $\sin\mu = 1/M$, and (X, Y) is a point on the Mach line [14, 15].

After some mathematical manipulations, the z-co-ordinate z_s of the point of the intersection of the above lines is given by

$$z_s = z + \frac{1}{h_1(z,x)u + h_2(z,x)} \tag{B3}$$

where

$$h_1(z,x) = [-4h^* M^2]/[(4 + h^{*2} x_5^2)(2\sqrt{M^2-1} + h^* x_5)]$$

$$h_2(z,x) = \frac{2M}{\sqrt{M^2-1}(2\sqrt{M^2-1} + h^* x_5)}$$

$$[1/(\sqrt{\gamma R x_3})\,\mathrm{d}v/\mathrm{d}z - v/(2\sqrt{\gamma R x_3^3})\,\mathrm{d}x_3/\mathrm{d}z]$$

The variable z_s is an increasing function of z in the compression region, and its positive minimum in this region is denoted by z_1.

APPENDIX C. THE SINGULAR PART OF THE NOZZLE SHAPE

A singular part of the nozzle appears when $\lambda_1 = \lambda_2 = \lambda_3 = 0$ on some interval. In this case, it follows from (20) that

$$p_5 \equiv 0 \tag{C1}$$

It is obvious that $\dot{p}_5$ is also zero on that interval and hence, by (22),

$$x_4 x_5 \dot{p}_5 = x_5 f_3 p_3 + x_5 x_4 p_4 = A_1 p_1 + A_2 p_2 + A_3 p_3 \equiv 0 \tag{C2}$$

Obviously, the first and the second derivatives of the above equation are also zero on that interval and thus

$$B_1 p_1 + B_2 p_2 + B_3 p_3 \equiv 0 \tag{C3}$$

$$(C_1 + D_1 u_s) p_1 + (C_2 + D_2 u_s) p_2 + (C_3 + D_3 u_s) p_3 \equiv 0 \tag{C4}$$

The above homogeneous system of linear equations (C2)–(C4) has non-zero solution if

$$\begin{vmatrix} A_1 & A_2 & A_3 \\ B_1 & B_2 & B_3 \\ C_1 + D_1 u_s & C_2 + D_2 u_s & C_3 + D_3 u_s \end{vmatrix} = 0 \tag{C5}$$

Then by solving the above equation with respect to u_s, the control function on the singular path, we have

$$u_s = -\frac{\begin{vmatrix} A_1 & A_2 & A_3 \\ B_1 & B_2 & B_3 \\ C_1 & C_2 & C_3 \end{vmatrix}}{\begin{vmatrix} A_1 & A_2 & A_3 \\ B_1 & B_2 & B_3 \\ D_1 & D_2 & D_3 \end{vmatrix}} \tag{C6}$$

where A_i, B_i, C_i, and D_i $(i = 1, 2, 3)$ are given as follows:

$$A_i = -f_i \tag{C7}$$

$$B_i = \sum_{j=1}^{3} \frac{\partial A_j}{\partial x_j} F_j + \sum_{j=1}^{3} A_j \frac{\partial F_j}{\partial x_i} \tag{C8}$$

$$C_i = \sum_{j=1}^{3} \frac{\partial B_j}{\partial x_j} F_j + \sum_{j=1}^{3} B_j \frac{\partial F_j}{\partial x_i} + \sum_{j=1}^{3} \left(-f_j B_j \frac{\partial F_j}{\partial x_4} \right) \tag{C9}$$

$$D_i = \frac{\partial B_i}{\partial x_5} \tag{C10}$$

APPENDIX D. TWO-DIMENSIONAL ANALYSIS

The governing equations (i.e. conservation of mass, momenta in y and z directions, and energy) are, respectively, as follows:

$$\frac{\partial \rho}{\partial t} + \frac{\partial}{\partial z}(\rho U_z) + \frac{\partial}{\partial y}(\rho U_y) = 0$$

$$\rho\left(\frac{\partial U_y}{\partial t} + U_y\frac{\partial U_y}{\partial y} + U_z\frac{\partial U_y}{\partial z}\right) = -\frac{\partial p}{\partial y}$$

$$\rho\left(\frac{\partial U_z}{\partial t} + U_y\frac{\partial U_z}{\partial y} + U_z\frac{\partial U_z}{\partial z}\right) = -\frac{\partial p}{\partial z}$$

$$\rho\left(\frac{\partial e}{\partial t} + U_y\frac{\partial e}{\partial y} + U_z\frac{\partial e}{\partial z}\right) = -p\frac{\partial U_y}{\partial y} - p\frac{\partial U_z}{\partial z}$$

where U_z and U_y are components of velocity, and T, p, ρ, and e are, respectively, the temperature, pressure, density, and energy. The z-axis is along the nozzle, and in the x-axis the nozzle has a constant profile.

For a two-dimensional gas flow, usually, this governing equations are rewritten in the conservative form [21]

$$\frac{\partial}{\partial t}\mathbf{A} + \frac{\partial}{\partial y}\mathbf{B} + \frac{\partial}{\partial z}\mathbf{C} = 0$$

where

$$\mathbf{A} = (\rho, \rho U_y, \rho U_z, E)$$

$$\mathbf{B} = (\rho U_y, p + \rho U_y^2, \rho U_y U_z, (E + p)U_y)$$

$$\mathbf{C} = (\rho U_z, \rho U_y U_z, p + \rho U_z^2, (E + p)U_z)$$

and $E = \rho(e + \frac{1}{2}(U_y^2 + U_z^2))$.

We use the following dimensionless variables:

$$y^* = y/l_0, \quad z^* = z/l_0, \quad t^* = t/(l_0/V_0) \quad U_y^* = U_y/(V_0), \quad U_z^* = U_z/V_0$$

$$\rho^* = \rho/\rho_0, \quad p^* = p/(\rho_0 V_0^2), \quad T^* = T/T_0, \quad e^* = e/V_0^2$$

where ρ_0, T_0, and $V_0 = \sqrt{\gamma R T_0}$ are values at throat, and l_0 is the total length of the computational region. Also the following non-uniform mesh, defined by y_1 and z_1, is used:

$$z_1 = (z^* d + \delta_1)^{\text{np}} + \delta_2, \quad y_1 = l_0 y^*/(f(z)h^*/2) \tag{C11}$$

where d, np, δ_1, and δ_2 are some parameters. (For Figure 8, we set $l_0 = 0.3$ m, $d = 11.12$, $\text{np} = 0.260577$, $\delta_1 = 0.0222285$, and $\delta_2 = -0.370888$.) Throughout the paper, $f(z)$ denotes the area ratio at position z.

Therefore

$$\frac{\partial z_1}{\partial z^*} = \frac{\text{np}\, d}{(z_1 - \delta_2)^{(1-\text{np})/\text{np}}}, \quad \frac{\partial z_1}{\partial y^*} = 0$$

$$\frac{\partial y_1}{\partial z^*} = -y_1 \frac{f'(z)}{f(z)}, \quad \frac{\partial y_1}{\partial y^*} = \frac{l_0}{(h^*/2) f(z)}$$

At last we have the following governing equations:

$$\frac{\partial}{\partial t^*}\mathbf{A}_1 + \left(\frac{l_0}{(h^*/2) f(z)}\right)\frac{\partial}{\partial y_1}\mathbf{B}_1 + \left(\frac{\text{np}\, d}{(z_1 - \delta_2)^{(1-\text{np})/\text{np}}}\frac{\partial}{\partial z_1} - y_1 \frac{f'(z)}{f(z)}\frac{\partial}{\partial y_1}\right)\mathbf{C}_1 = 0$$

where $\mathbf{A}_1$, $\mathbf{B}_1$, and $\mathbf{C}_1$ are the same as $\mathbf{A}$, $\mathbf{B}$, and $\mathbf{C}$ in which the flow quantities are replaced by their corresponding dimensionless variables. The latter equations are rewritten in the form

$$\frac{\partial}{\partial t^*}\mathbf{q} + \frac{\partial}{\partial y_1}\mathbf{F} + \frac{\partial}{\partial z_1}\mathbf{G} + \mathbf{H} = 0$$

where

$$\mathbf{q} = \mathbf{A}_1$$

$$\mathbf{F} = [l_0/(h^*/2 f(z))]\mathbf{B}_1 - [y_1 f'(z)/f(z)]\mathbf{C}_1$$

$$\mathbf{G} = (\text{np} - 1) d (z_1 - \delta_2)^{-1/\text{np}} \mathbf{C}_1$$

$$\mathbf{H} = [f'(z)/f(z)]\mathbf{C}_1$$

To solve these equations through the nozzle, the following boundary conditions are applied:
At $z_1 = 0$, $T = 1$, $U_y = 0$, $U_z = 1$, $\rho = 1$, and $p = 1/\gamma$.
At $z_1 = 1$, we use extrapolations $\partial U_z/\partial z_1 = 0$, $\partial U_y/\partial z_1 = 0$, $\partial \rho/\partial z_1 = 0$, and $\partial \rho/\partial z_1 = 0$.
For points with $y_1 = 0$, $U_y = 0$, $\partial U_z/\partial y_1 = 0$, $\partial p/\partial y_1 = 0$, $\partial \rho/\partial y_1 = 0$.
Finally, at $y_1 = 1$, we use conditions $U_y = 0$, $U_z = 0$, and $\partial p/\partial y_1 = 0$.

The numerical solution in two-dimensional grid is obtained by a two gird type of MacCormack method [21].

REFERENCES

1. Anderson Jr JD. *Gasdynamic Lasers*: *An Introduction*. Academic Press: New York, 1976.
2. Losev SV, Makarov VN. Optimization of the gain of a carbon dioxide gas-dynamic laser. *Soviet Journal of Quantum Electronics* 1975; **4**:905.
3. Losev SV, Makarov VN. Multifactor optimization of a carbon dioxide gasdynamic laser. I. Gain optimization. *Soviet Journal of Quantum Electronics* 1975; **5**:780.
4. Losev SV, Makarov VN. Multifactor optimization of a carbon dioxide gasdynamic laser. II. Specific power optimization. *Soviet Journal of Quantum Electronics* 1976; **6**:514.
5. Reddy NM, Shanmugasundaram V. Theoretical gain-optimization studies in CO_2–N_2 gasdynamic lasers. I. Theory. *Journal of Applied Physics* 1979; **50**:2565.
6. Reddy NM, Shanmugasundaram V. Theoretical gain-optimization studies in CO_2–N_2 gasdynamic lasers. II. Results of parametric study. *Journal of Applied Physics* 1979; **50**:2576.

7. Reddy KPJ, Reddy NM. Theoretical gain optimization studies in 10.6 μm CO_2–N_2 gasdynamic lasers. IV. Further results of parametric study. *Journal of Applied Physics* 1984; **55**:51.
8. Biryukov AS, Karakhanova IV, Konoplev NA, Shcheglev VA. Thermally excited CO_2 cascade lasers. *Soviet Journal of Quantum Electronics* 1984; **13**:1631.
9. Bahrampour AR, Radjabalipour M. On optimal nozzle shapes of gas-dynamic lasers. *Journal of Sciences, Islamic Republic of Iran* 1996; **7**:181.
10. Shojaei M, Bolorizadeh MA, Bahrampour AR, Rahnama M, Mehdezadeh E. Effect of nozzle shape on small signal gain in gasdynamic laser. *Proceedings of the Gas Flow and Chemical Lasers* 1992; **SPIE-1810**:334.
11. Kanazova H, Saito H, Yamada H, Masuda W, Kasuya K. Theoretical analysis of combustion-driven 16 μm CO_2 gasdynamic lasers. *IEEE Journal of Quantum Electronics* 1984; **QE-20**:1086.
12. Losev SA. *Gasdynamic Lasers*. Springer: New York, 1981.
13. Vincenti WG, Kruger Jr CH. *Introduction to Physical Gasdynamics*. Wiley: New York, 1965.
14. Shapiro AH. *The Dynamics and Thermodynamics of Compressible Fluid Flow*. Ronald Press: New York, 1954.
15. Landau LD, Lifshits EM. *Fluid Mechanics*. Pergamon Press: New York, 1987.
16. Blanchard P, Bruning E. *Variational Methods in Mathematical Physics: A Unified Approach* (translated by: Hayes G.M.). Springer: New York, 1992.
17. Katalkherman MG, Mal'kov VM, Petekhov AV, Kharitanova YaI. Gain of a gasdynamic laser utilizing products of benzene combustion. *Soviet Journal of Quantum Electronics* 1977; **7**:97.
18. Tatsumi M, Wada Y, Sato S, Watanuki T, Kubota H. Numerical analysis on gain of C_6H_6–O_2–N_2 type GDL. *Proceedings of the Seventh Gas Flow and Chemical Lasers* 1988; **SPIE-1031**:166.
19. Watanuki T, Sato S, Itakura Y, Ogura E, Mizobuchi Y, Kubota H. Characteristics of C_6H_6–O_2–N_2 type CO_2 gasdynamic laser. *Proceedings of the Seventh Gas Flow and Chemical Lasers* 1988; **SPIE-1031**:160.
20. Sato S, Watanuki T, Matsuzaka M, Yamaguchi M, Kubota H. Gain of a gasdynamic laser utilizing products of liquid C_6H_6 and gaseous O_2 combustion. *Proceedings of the Sixth Gas Flow and Chemical Lasers*. Proceedings in Physics, vol. 15. Springer: Berlin, New York, 1986; 301.
21. Anderson DA, Tannehill JC, Pletcher RH. *Computational Fluid Mechanics and Heat Transfer*. Hemisphere Publishing Co: New York, 1984.

